Electronic Supplementary Information

Constructing Perfect Cubic Ag-Cu Alloyed Nanoclusters through Selective Elimination of Phosphine Ligands

Li Tang,[a,‡] Qikai Han,[a,‡] Bin Wang[a], Zhonghua Yang,[b] Chunyuan Song,[a] Guanyu Feng,[a] and Shuxin Wang*[a]

[a]*College of Materials Science and Engineering, Qingdao University of Science and Technology, Qingdao 266042, P. R. China.*

[b] *College of Chemistry and Molecular Engineering, Qingdao University of Science and Technology, Qingdao 266042, P. R. China.*

*E-mail of corresponding author: shuxin_wang@qust.edu.cn

Table of Contents

Section 1. Experimental Procedures

Characterization

Materials and Synthesis

Section 2. Supplementary Figures

Fig. S1 An optical microscopic image of the single crystals of **$Ag_{55}Cu_8I_{12}$**.

Fig. S2 X-ray photoelectron spectroscopy (XPS) of **$Ag_{55}Cu_8I_{12}$**.

Fig. S3 SEM image and energy-dispersive X-ray spectrum(EDX) of **$Ag_{55}Cu_8I_{12}$**.

Fig. S4 The thermogravimetric analysis (TGA) results of **$Ag_{55}Cu_8I_{12}$** under a N_2 atmosphere.

Fig. S5 ^{31}P-NMR spectrum of **$Ag_{55}Cu_8I_{12}$**.

Fig. S6 ^{1}H-NMR spectrum of **$Ag_{55}Cu_8I_{12}$**.

Fig. S7 ^{1}H-NMR spectrum of PPh_4Br.

Fig. S8 Energy scale spectra of (a) **$Ag_{55}Cu_8I_{12}$** and (b) **Ag_{63}**.

Fig. S9 The overall structure of the **$Ag_{55}Cu_8I_{12}$**.

Fig. S10 Comparing the deviations in the edges of the cubic structures between **$Ag_{55}Cu_8I_{12}$** and **Ag_{63}**.

Fig. S11 UV-Vis spectra of 1,2-dichloroethane solutions of **$Ag_{55}Cu_8I_{12}$** heated in air at 50℃ for different times.

Fig. S12 Packing of the **$Ag_{55}Cu_8I_{12}$** and **Ag_{63}** in crystal lattices.

Section 3. Supplementary Tables

Table S1 Crystal data and structure refinement for the **$Ag_{55}Cu_8I_{12}$**.

Table S2 The atomic ratio of Ag and Cu in **$Ag_{55}Cu_8I_{12}$** was calculated from XPS, ICP and EDX measurements.

Table S3 Comparison of different bond lengths in **$Ag_{55}Cu_8I_{12}$** and **Ag_{63}** crystal structures.

Table S4 Comparing the bond lengths deviations on the edges of the cubic structures between **$Ag_{55}Cu_8I_{12}$** and **Ag_{63}**.

Table S5 Comparing the angular deviations on the edges of the cubic structures between **$Ag_{55}Cu_8I_{12}$** and **Ag_{63}**.

Section 4. References

1. Experimental Procedures

Characterization

The UV-Vis absorption spectra of nanoclusters were performed on UV-8000 spectrophotometer. X-ray photoelectron spectroscopy (XPS) measurements were acquired an ESCALAB XI+, with a mono chromate AlKα (1486.8 eV) 150 W X-ray source, 0.5 mm circular spot size, a flood gun to counter charging effects, and analysis chamber base pressure lower than 1 x 10^{-9} mbar. A Scanning Electron Microscope (SEM) analysis was performed using an */S-4800 microscope, which operated within an accelerating voltage range of 0.1-30 kV. Nuclear magnetic resonance (NMR) measurements were performed on a Bruker Avance II spectrometer. For ^{1}H and ^{31}P NMR, CD_2Cl_2 was used as the solvent to dissolve all crystal samples. Inductively coupled plasma atomic emission spectrometry (ICP-AES) measurements were collected on an AtomScan Advantage instrument made by Thermo Jerrell Ash Corporation. Thermo gravimetric analysis (TGA) was carried out on ST 8000, 5 mg of the nanocluster at a heating rate of 10 K min^{-1} from room temperature to 773.15K.

The SC-XRD data of the **$Ag_{55}Cu_8I_{12}$** nanoclusters was collected using a Bruker D8 QUEST X-ray single-crystal diffractometer with Mo Kα radiation (λ = 0.71073 Å) at 170K. The nanocluster structures were solved using the ShelXT structure solution program via intrinsic phasing in Olex2. Subsequently, the full matrix least squares method was used to improve the structure of F^2 using the SHELXTL software package.

Materials

Silver nitrate ($AgNO_3$; ≥99.99%; metal basis), copper iodide (CuI; >99.99%, metal basis), Triphenylphosphine (PPh_3, 99%), Tetraphenyl phosphorus bromide (BrPPh; 99%), 2,4-dimethylbenzenethiol (HS-$C_6H_3^{2,4}(CH_3)_2$; 98%), sodium borohydride ($NaBH_4$; ≥99%, Aldrich), triethylamine ($C_6H_{15}N$, ≥99%, Aldrich), *n*-hexane (C_6H_{14}, Hex; ≥99%, Aldrich), dichloromethane (CH_2Cl_2; ≥99%, Aldrich) and methanol (CH_3OH; ≥99%, Aldrich) were used in the experiments. All chemicals are commercially available and used as received.

Synthesis of the $Ag_{55}Cu_8I_{12}$ nanocluster

The preparation of **$Ag_{55}Cu_8I_{12}$** was based on the method reported by Zheng's group with minor modifications.[S1] $AgNO_3$ (40 mg) was dissolved in a mixture solution containing 3 mL of methanol and 10 mL of CH_2Cl_2 under vigorously stirred. After stirring for 2 minutes, 50 mg of PPh_3, 20 mg of PPh_4Br, and 163 µL of 2, 4-dimethylbenzenethiol (HS-$C_6H_3^{2,4}(CH_3)_2$) was added to the reaction mixture in turn, which was vigorously stirred for an additional 15 minutes. CuI (25 mg) was introduced to the reaction solution. A freshly prepared solution of $NaBH_4$ (160 mg) and 100 µL of triethylamine dissolved in 2 mL of ice-cold pure water was quickly added to the reaction mixture, causing the light yellow solution to immediately darken. The reaction was allowed to proceed for 12 hours. Finally, the solution was concentrated to 4 mL using a rotary evaporator and washed multiple times with excess MeOH to remove excess thiolate. This extraction process was repeated several times. The resulting solution was then centrifuged to obtain a solid precipitate, which was dissolved in CH_2Cl_2, resulting in a solution of **$Ag_{55}Cu_8I_{12}$** nanoclusters. Crystallization was subsequently performed in a mixed solution of CH_2Cl_2 and *n*-hexane at 4°C. After approximately one week (Fig. S1), crystals of **$Ag_{55}Cu_8I_{12}$** were obtained with a yield of approximately 56% based on the silver content.

2. Supplementary Figures

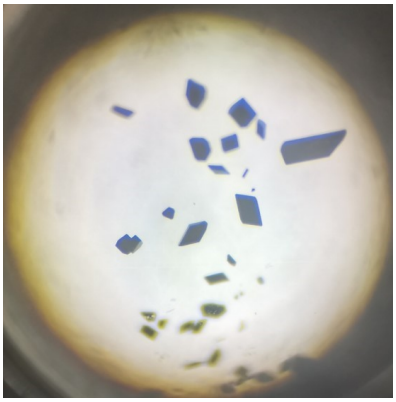

Fig. S1 An optical microscopic image of the single crystals of **$Ag_{55}Cu_8I_{12}$**.

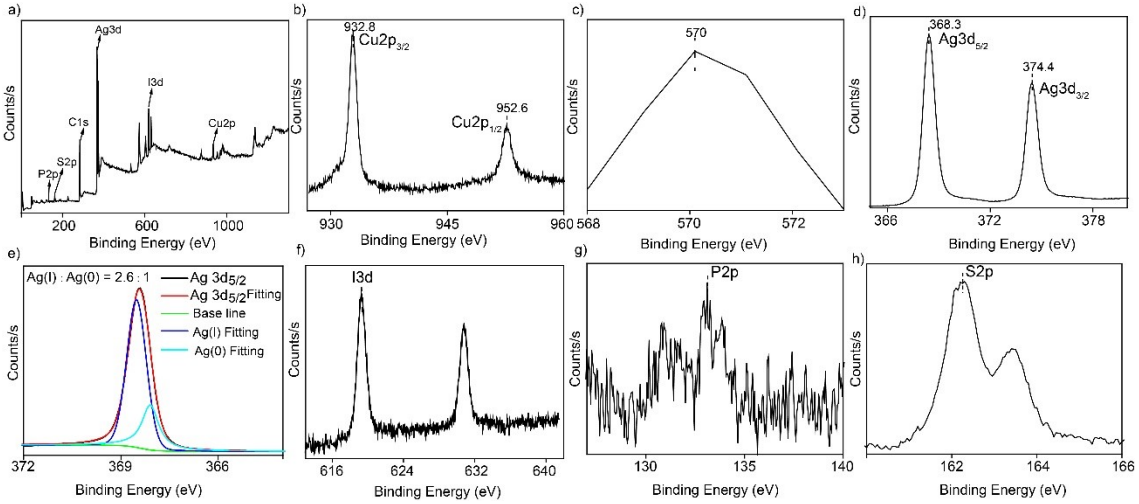

Fig. S2 X-ray photoelectron spectroscopy (XPS) of **$Ag_{55}Cu_8I_{12}$**. a) XPS, b) Cu 2p, c) Cu LMM, d) Ag 3d, e) XPS of measured Ag $3d_{5/2}$ (black curve), fitting line of Ag $3d_{5/2}$ (red curve), base line (green curve), fitting line of Ag (I) (blue curve) and fitting line of Ag (0) (turquiose curve). f) I 3d, g) P 2p, h) S 2p.

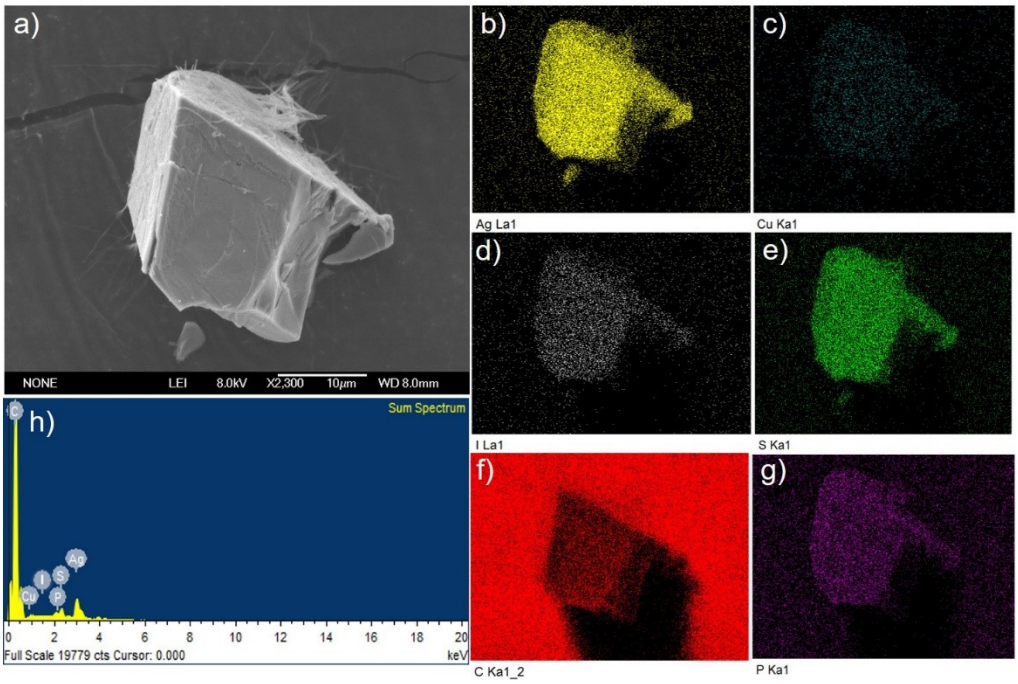

Fig. S3 (a) SEM image of a small deformed single crystal of **$Ag_{55}Cu_8I_{12}$**. (b-g) are the elemental maps of Ag, Cu, I, S, C, and P, respectively. (h) EDX spectrum, confirming the presence of the above elements in the cluster, which is consistent with the cluster composition obtained by SCXRD data.

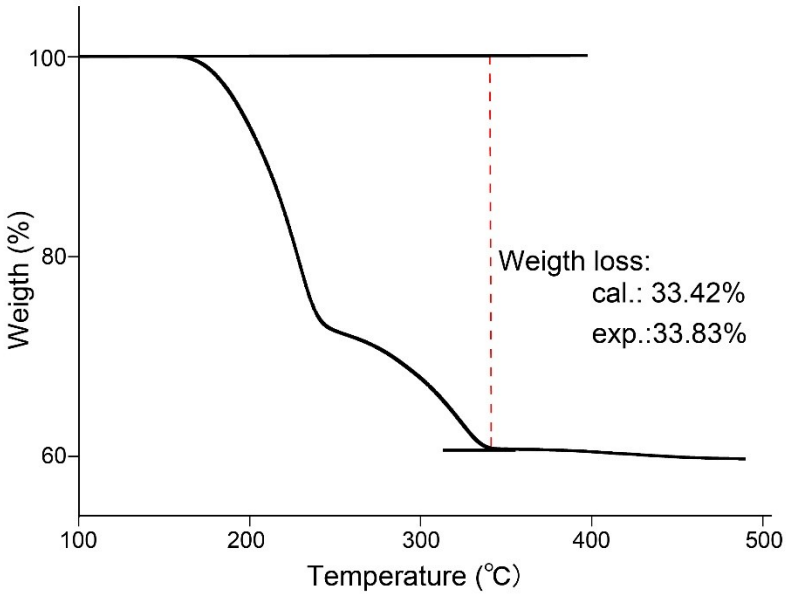

Fig. S4 The thermogravimetric analysis (TGA) results of **$Ag_{55}Cu_8I_{12}$** under a N_2 atmosphere.

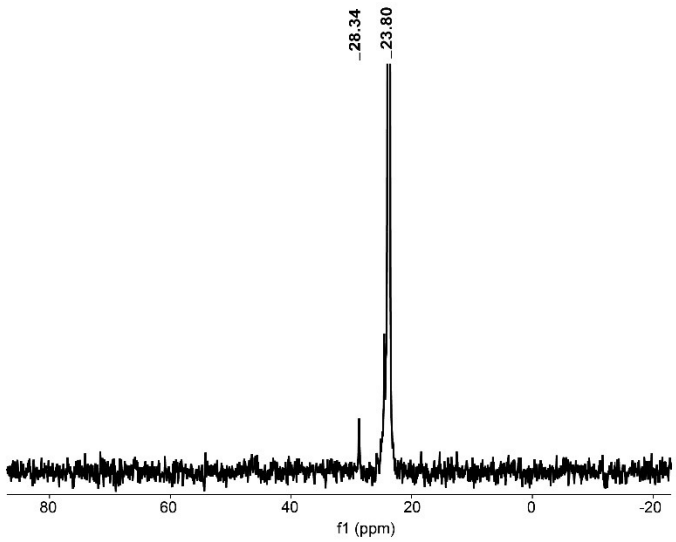

Fig. S5 ^{31}P-NMR spectrum of $\mathbf{Ag_{55}Cu_8I_{12}}$.

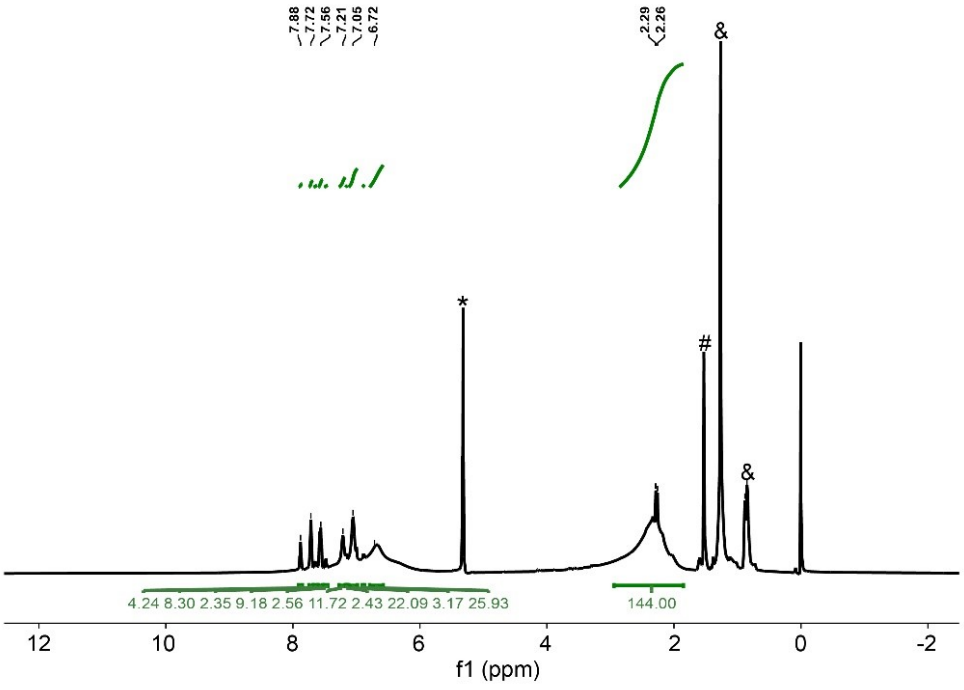

Fig. S6 ^{1}H-NMR spectrum of $\mathbf{Ag_{55}Cu_8I_{12}}$. Notes: * = CD_2Cl_2; # = H_2O; & = n-hexane.

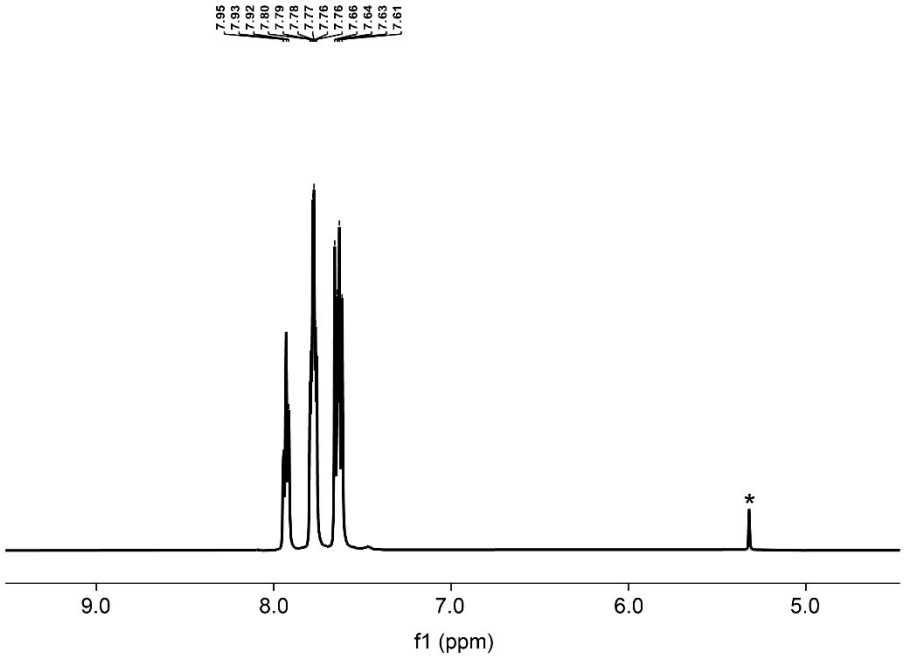

Fig. S7 ^{1}H-NMR spectrum of PPh_4Br. Notes: * stands for CD_2Cl_2.

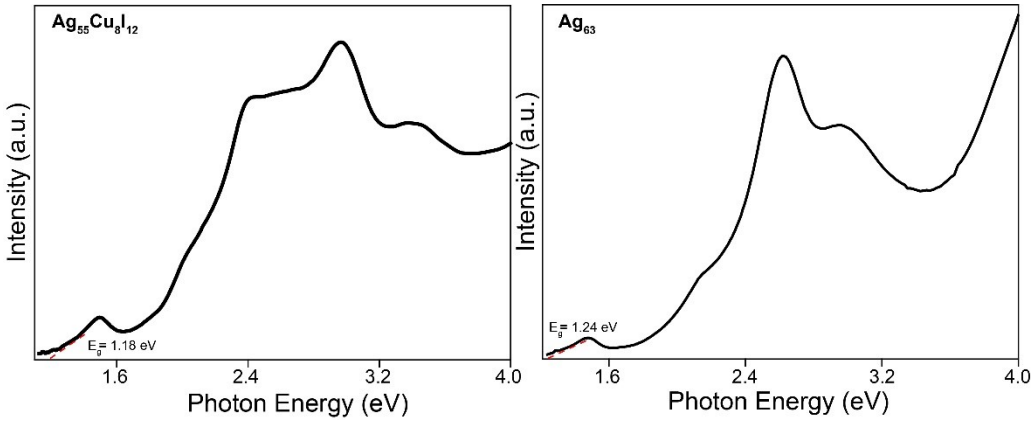

Fig. S8 Energy scale spectra of (a) **$Ag_{55}Cu_8I_{12}$** and (b) **Ag_{63}**.

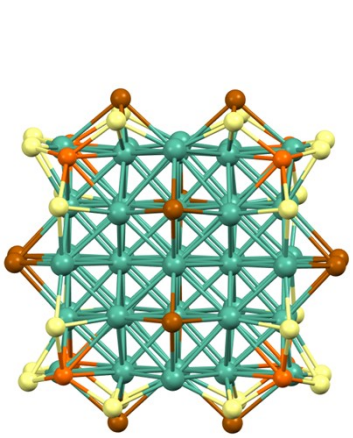

Fig. S9 The overall structure of the $Ag_{55}Cu_8I_{12}$. Color legends: Ag = dark green, Cu = orange, S = yellow, I = brown, P = magenta. For clarity, C and H atoms are all omitted.

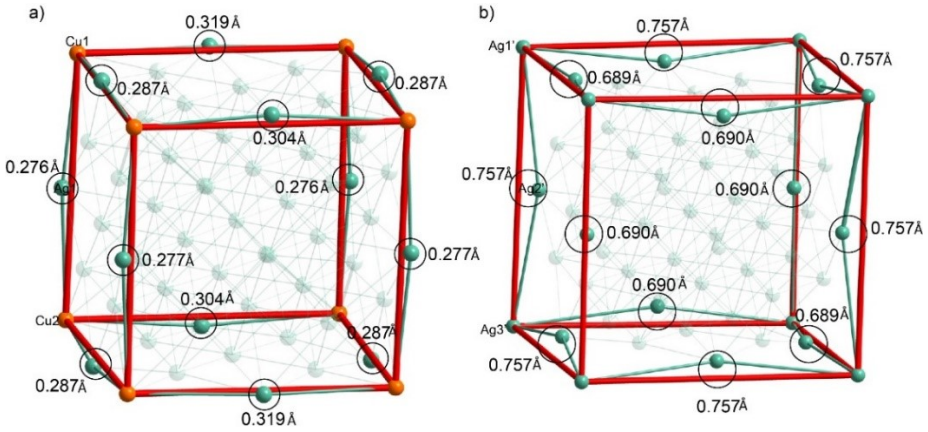

Fig. S10 Comparing the deviations in the edges of the cubic structures between (a) $Ag_{55}Cu_8I_{12}$ and (b) Ag_{63}.

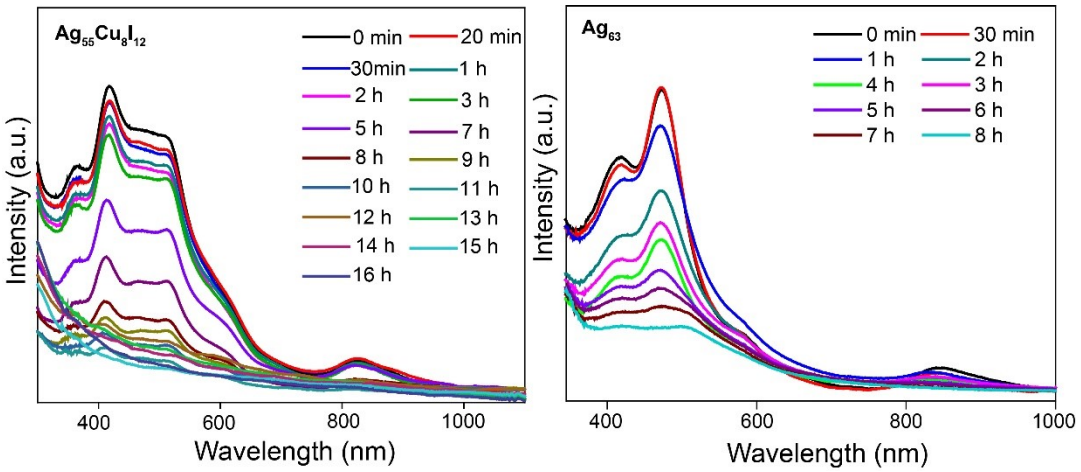

Fig. S11 UV-Vis spectra of 1,2-dichloroethane solutions of (a) **$Ag_{55}Cu_8I_{12}$** and (b) **Ag_{63}** heated in air at 50℃ for different times.

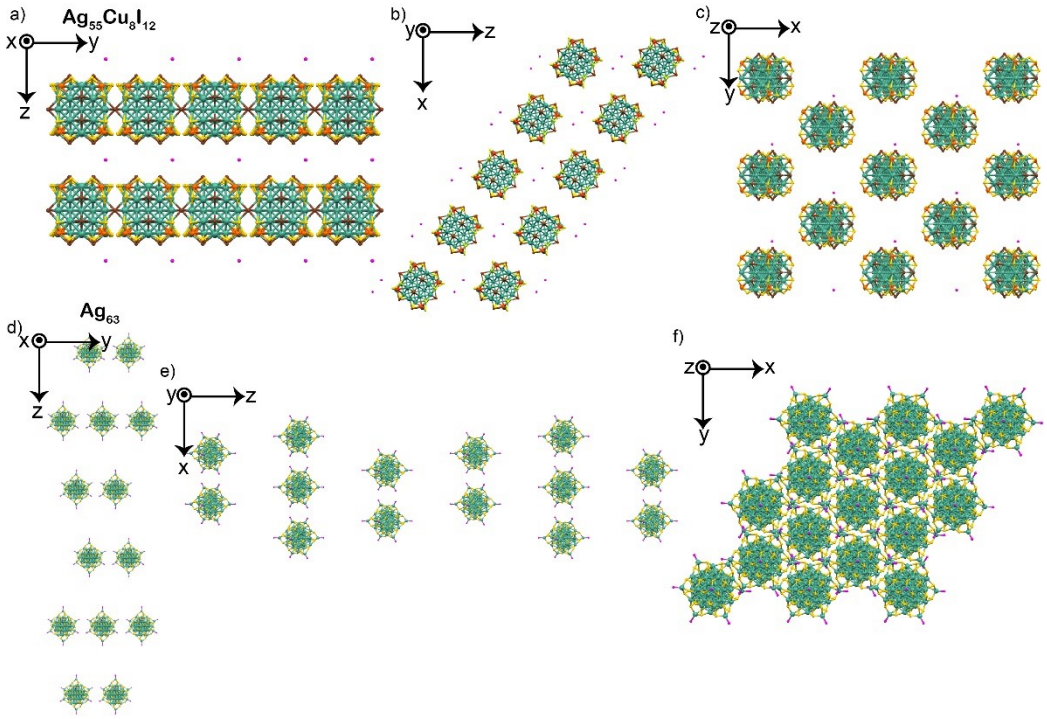

Fig. S12 Panels (a-c) illustrate the packing of **$Ag_{55}Cu_8I_{12}$** and panels (d-f) show **Ag_{63}** within crystal lattices, viewed from the x-axis (a, d), y-axis (b, e), and z-axis (c, f). The color legend is as follows: Ag in dark green, Cu in orange, S in yellow, I in brown, and P in magenta. For enhanced clarity, carbon and hydrogen atoms have been omitted.

3. Supplementary Tables

Table S1 Crystal data and structure refinement for the $Ag_{55}Cu_8I_{12}$.

Empirical formula	$C_{216}H_{236}Ag_{55}I_{12}Cu_8PS_{24}$
Formula weight	11596.41
Temperature/K	170
Crystal system	monoclinic
Space group	C2/m
Unit cell dimensions	a = 37.341(5) Å α= 90 °
	b = 24.083(3) Å β= 125.295(2) °
	c = 22.341(3) γ= 90°
Volume/Å^3	16398(4)
Z	2
ρ calcg/cm3	2.349
μ /mm-1	5.023
F(000)	10768.0
Crystal size/mm3	0.07 × 0.05 × 0.05
Radiation	MoKα (λ = 0.71073)
2θ range for data collection/°	4.084 to 52.778
Index ranges	-46 ≤ h ≤ 41, -30 ≤ k ≤ 29, -27 ≤ l ≤ 27
Reflections collected	35734
Independent reflections	16890 [Rint = 0.0635, Rsigma = 0.0935]
Data/restraints/parameters	16890/3224/1162
Goodness-of-fit on F2	0.925
Final R indexes [I>=2σ (I)]	R_1 = 0.0710, wR_2 = 0.1992
Final R indexes [all data]	R_1 = 0.1541, wR_2 = 0.2576
Largest diff. peak/hole / e Å^{-3}	2.13/-0.79

Table S2 The atomic ratio of Ag and Cu in **$Ag_{55}Cu_8I_{12}$** was calculated from X-ray photoelectric spectroscopy (XPS), inductively coupled plasma (ICP) and energy-dispersive X-ray spectrum (EDX) measurements.

Measurement	Ag(%)	Cu(%)
XPS results	86.9	13.1
ICP results	87.2	12.8
EDX results	86.5	13.5
Theoretical results	55/63 (87.3)	8/63(12.7)

Table S3 Comparison of different bond lengths in **$Ag_{55}Cu_8I_{12}$** and **Ag_{63}** crystal structures.

Cluster / Bond length (Å)	$Ag_{55}Cu_8I_{12}$			Ag_{63}		
	min.	max.	average	min.	max.	average
Ag(C)-Ag(SS)	2.883	2.886	2.885	2.878	2.897	2.886
Ag(SS)-Ag(SS)	2.877	2.893	2.886	2.845	2.963	2.886
Ag(SS)-Ag(S)	2.806	3.152	2.904	2.835	3.267	2.938
Ag(S)-Ag(S)	2.811	3.241	2.953	2.852	3.178	2.982
Ag-Cu	2.85	3.003	2.904	-	-	-
Cu-S	2.24	2.325	2.287	-	-	-
Ag-I	2.826	2.968	2.894	-	-	-
Ag-S	2.461	2.739	2.581	2.495	2.74	2.587
Ag-P	-	-	-	2.394	2.406	2.392

Notes:

Ag(S) stands for the surface silver atom covered by thiolate;

Ag(SS) stands for the subsurface Ag atom adjacent to the surface Ag atom;

Ag(C) stands for the central Ag atom.

Tabel S4 Comparing the bond length deviations on the edges of the cubic structures between **$Ag_{55}Cu_8I_{12}$** and **Ag_{63}**.

Cluster / Bond length (Å)	$Ag_{55}Cu_8I_{12}$	Ag_{63}	$Ag_{55}Cu_8I_{12}$ diff. (Å) i.e. 4.122+3.998-8.01	Ag_{63} diff. (Å) i.e. 4.838+4.796-9.514
Cu1-Ag1 (Ag1'-Ag2')	4.122	4.838	0.019	0.12
Ag1-Cu2 (Ag2'-Ag3')	3.998	4.796		
Cu1-Cu2 (Ag1'-Ag3')	8.101	9.514		
Cu7-Ag7 (Ag13'-Ag14')	4.122	4.838	0.019	0.12
Ag7-Cu8 (Ag14'-Ag15')	3.998	4.796		
Cu7-Cu8 (Ag13'-Ag15')	8.101	9.514		
Cu1-Ag4 (Ag1'-Ag8')	4.006	4.953	0.02	0.097
Ag4-Cu4 (Ag8'-Ag7')	4.204	4.795		
Cu1-Cu4 (Ag1'-Ag7')	8.19	9.651		
Cu2-Ag2 (Ag3'-Ag4')	4.006	4.838	0.02	0.12
Ag2-Cu3 (Ag4'-Ag5')	4.204	4.796		
Cu2-Cu3 (Ag3'-Ag5')	8.19	9.514		
Cu4-Ag3 (Ag7'-Ag6')	3.998	4.797	0.019	0.097
Ag3-Cu3 Ag6'-Ag5')	4.122	4.953		
Cu4-Cu3 (Ag7'-Ag5')	8.101	9.653		
Cu6-Ag5 (Ag11'-Ag10')	3.998	4.797	0.019	0.097
Ag5-Cu5 (Ag10'-Ag9')	4.122	4.953		
Cu6-Cu5 (Ag11'-Ag9')	8.101	9.653		
Cu6-Ag6 (Ag11'-Ag12')	4.204	4.795	0.02	0.097
Ag6-Cu7 (Ag12'-Ag13')	4.006	4.953		
Cu6-Cu7 (Ag11'-Ag13')	8.19	9.651		
Cu5-Ag8 (Ag9'-Ag16')	4.204	4.796	0.02	0.12
Ag8-Cu8 (Ag16'-Ag15')	4.006	4.838		
Cu5-Cu8 (Ag9'-Ag15')	8.19	9.514		
Cu2-Ag11 (Ag3'-Ag19')	4.121	4.953	0.022	0.098
Ag11-Cu6 (Ag19'-Ag11')	4.121	4.796		
Cu2-Cu6 (Ag3'-Ag11')	8.22	9.651		
Cu8-Ag10 (Ag15'-Ag18')	4.121	4.953	0.022	0.098
Ag10-Cu4 (Ag18'-Ag7')	4.121	4.796		
Cu8-Cu4 (Ag15'-Ag7')	8.22	9.651		
Cu3-Ag12 (Ag5'-Ag20')	4.044	4.838	0.025	0.12
Ag12-Cu7 (Ag20'-Ag13')	4.044	4.796		
Cu3-Cu7 (Ag5'-Ag13')	8.063	9.514		
Cu5-Ag9 (Ag9'-Ag17')	4.044	4.838	0.025	0.12
Ag9-Cu1 (Ag17'-Ag1')	4.044	4.796		
Cu5-Cu1 (Ag9'-Ag1')	8.063	9.514		

Table S5 Comparing the angular deviations on the edges of the cubic structures between **$Ag_{55}Cu_8I_{12}$** and **Ag_{63}**.

Cluster / Bond angle (◦)	$Ag_{55}Cu_8I_{12}$	Ag_{63}	$Ag_{55}Cu_8I_{12}$	Ag_{63}
			diff. (%)	diff.(%)
			i.e. (180-172.17)/180	i.e. (180-161.89)/180
Cu1-Ag1-Cu2 (Ag1'-Ag2'-Ag3')	172.17	161.89	4.35	10.06
Cu7-Ag7-Cu8 (Ag13'-Ag14'-Ag15')	172.17	161.89	4.35	10.06
Cu1-Ag4-Cu4 (Ag1'-Ag8'-Ag7')	171.97	163.72	4.46	9.04
Cu2-Ag2-Cu3 (Ag3'-Ag4'-Ag5')	171.97	161.89	4.46	10.06
Cu4-Ag3-Cu3 (Ag7'-Ag6'-Ag5')	172.17	163.73	4.35	9.04
Cu6-Ag5-Cu5 (Ag11'-Ag10'-Ag9')	172.17	163.73	4.35	9;04
Cu6-Ag6-Cu7 (Ag11'-Ag12'-Ag13')	171.97	163.72	4.46	9.04
Cu5-Ag8-Cu8 (Ag9'-Ag16'-Ag15')	171.97	161.89	4.46	10.06
Cu2-Ag11-Cu6 (Ag3'-Ag19'-Ag11')	171.52	163.71	4.71	9.05
Cu8-Ag10-Cu4 (Ag15'-Ag18'-Ag7')	171.52	163.71	4.71	9.05
Cu3-Ag12-Cu7 (Ag5'-Ag20'-Ag13')	170.94	161.89	5.03	10.06
Cu5-Ag9-Cu1 (Ag9'-Ag17'-Ag1')	170.94	161.89	5.03	10.06

4. References

[S1] H. Yang, J. Yan, Y. Wang, H. Su, L. Gell, X. Zhao, C. Xu, B. K. Teo, H. Hakkinen and N. Zheng, *J. Am. Chem. Soc.*, 2017, **139**, 31-34.